THE JOURNAL OF BIOLOGICAL CHEMISTRY
Vol. 276, No. 47, Issue of November 23, pp. 43635–43644, 2001
Printed in U.S.A.

High Affinity Association of *myo*-Inositol Trisphosphates with Phytase and Its Effect upon the Catalytic Potential of the Enzyme*

Received for publication, August 7, 2001, and in revised form, August 28, 2001
Published, JBC Papers in Press, August 29, 2001, DOI 10.1074/jbc.M107531200

Usha Padmanabhan‡, Shashiprabha Dasgupta§, Birendra B. Biswas§, and Dipak Dasgupta‡¶

From the ‡Biophysics Division, Saha Institute of Nuclear Physics, 37 Belgachia Road, Kolkata 700 037 and §Biophysics and Molecular Biology Department, University of Calcutta, Kolkata 700 009, India

A neutral phytase from germinating mung bean (*Vigna radiata*) seeds dephosphorylates *myo*-inositol hexakisphosphate sequentially to *myo*-inositol. The enzyme also binds with higher affinity to *myo*-inositol trisphosphates (1,4,5), (2,4,5), and (1,3,4) isomers without catalysis. The high affinity complex elicits Ca^{2+} mobilization *in vitro* from microsomes/vacuoles via the formation of a ternary complex with the receptor for Ins(1,4,5)P_3. As a sequel to our previous report, we have carried out a detailed characterization of the two sites and examined the mutual interactions between them. Presaturation of the high affinity site leads to an increase in the affinity of the enzyme for phytic acid and its rate of dephosphorylation as well. From the products of limited tryptic cleavage of phytase, two peptides, each with one activity, have been isolated. The larger peptide (~66 kDa) contains the catalytic site, and the smaller peptide (~5 kDa) has the high affinity *myo*-inositol trisphosphate-binding site. The interaction between the dual activities of phytase has been observed also at the level of the two peptides. A sequence homology search using N-terminal 12 amino acid residues of the 5-kDa fragment has revealed significant homology with the Homer class of proteins implicated in signaling pathways involving metabotropic glutamate receptor and *myo*-inositol 1,4,5-trisphosphate receptor. These results indicate a second role of phytase in Ca^{2+} mobilization during germination of mung been seed via a salvage pathway that involves allosteric activation by *myo*-inositol trisphosphate.

Phytase (D-*myo*-inositol hexakisphosphate hydrolase) from mung bean seed, *Vigna radiata,* is a neutral phosphatase that dephosphorylates *myo*-inositol hexakisphosphate, $InsP_6$,[1] in the following sequential way: $InsP_6 \rightarrow InsP_5 \rightarrow InsP_4 \rightarrow InsP_3 \rightarrow InsP_2 \rightarrow InsP \rightarrow Ins$. It is ubiquitous in its occurrence. Its amount increases during the germination of seed (1). Phytase isolated from 72-h germinating mung bean seeds is a monomeric enzyme of molecular mass of 160 kDa with a pH optimum of 7.5 (2). A previous study (3) has demonstrated that in the sequential dephosphorylation of $InsP_6$, the enzyme displays increasing affinity for the substrate, $InsP_n$ (n = 1–6), with a decrease in the number of phosphate groups. Binding of the substrates at the catalytic site in phytase is characterized by dissociation constants in the micromolar range (3). This report (3) showed the presence of a high affinity (dissociation constant in the nanomolar order) non-catalytic site, specific for Ins(1,4,5)/(2,4,5)/(1,3,4)P_3, in phytase. Phytase-*myo*-inositol trisphosphate complex formed at the high affinity site forms a ternary complex with the putative receptor for Ins(1,4,5)P_3 and enhances the level of calcium release from microsomal/vacuolar suspension *in vitro*. The amount of calcium mobilized by the high affinity complex was about three times greater than that released by *myo*-inositol trisphosphate alone. Another interesting observation was that the complex formation at the high affinity site also activates otherwise inactive Ins(1,3,4)P_3 for calcium mobilization from vacuoles/microsomes (3).

These results imply that the high affinity $InsP_3$-binding site is distinct from the catalytic site and has an important physiological role. Therefore, we examined the influence of the high affinity $InsP_3$ binding to phytase on its substrate binding and hydrolyzing activity involving the catalytic site. Present studies suggest that saturation of the high affinity binding site with Ins(1,4,5)/(2,4,5)/(1,3,4)P_3 leads to an increase in the affinity of the enzyme for $InsP_6$. It is associated with a concurrent increase in the rate of hydrolysis of $InsP_6$ by phytase. In order to find a molecular explanation of the above observation, we have also carried out an enzymatic dissection of phytase using trypsin. The results conclusively illustrate that the two sites are functionally non-overlapping and distinct.

Signal-activated hydrolysis of PtdIns(4,5)P_2 by phospholipase C is the only known pathway of the production of *myo*-inositol trisphosphate (Ins(1,4,5)P_3), a well known second messenger that manifests many of its effects by inducing intracellular Ca^{2+} mobilization in eukaryotic systems (4, 5). Low levels of PtdIns(4,5)P_2 and a large excess of $InsP_6$ in seeds seem to suggest the existence of an alternative pathway for the production of inositol trisphosphate ($InsP_3$) in plants (6, 7). The previous report (3) indicates the presence of such an alternate pathway, which leads to production of inositol trisphosphates. The results presented here further support the presence of such an alternate pathway. We have also noticed a significant homology between Homer, a protein implicated in signaling pathway (8), and the N-terminal amino acid sequence of a tryptic fragment (5 kDa) that contains the high affinity site for binding to Ins(1,4,5)P_3 and mobilizes Ca^{2+} from microsomes/vacuoles isolated from the hypocotyls of germinating mung bean seeds. Below we have discussed the significance of the results *vis-à-vis* an alternate pathway of production of *myo*-inositol trisphosphate involving phytase and its biological role during germination of mung bean seeds.

* The costs of publication of this article were defrayed in part by the payment of page charges. This article must therefore be hereby marked "*advertisement*" in accordance with 18 U.S.C. Section 1734 solely to indicate this fact.

¶ To whom correspondence should be addressed: Biophysics Division, Saha Institute of Nuclear Physics, 37 Belgachia Rd., Calcutta 700 037. Tel.: 91-33-5565611; Fax: 91-33-3374637; E-mail: dipak@biop.saha.ernet.in.

[1] The abbreviations used are: $InsP_6$, D-*myo*-inositol hexakisphosphate or phytic acid; PtdInsP_2, phosphatidylinositol 4,5-bisphosphate; Ins(1,4,5)P_3, D-*myo*-inositol 1,4,5-trisphosphate; Ins(2,4,5)P_3, D-*myo*-inositol 2,4,5-trisphosphate; Ins(1,3,4)P_3, D-*myo*-inositol 1,3,4-trisphosphate; $InsP_3$, any of the isomers Ins(1,4,5)/(2,4,5)/(1,3,4)P_3; bis-ANS, 4,4′-dianilino-1,1′-binaphthyl-5,5′-disulfonic acid; $InsP_3$R, receptor for Ins(1,4,5)P_3; PAGE, polyacrylamide gel electrophoresis.

EXPERIMENTAL PROCEDURES

$InsP_6$, $Ins(1,4,5)P_3$, $Ins(2,4,5)P_3$, $Ins(1,3,4)P_3$, trypsin, polyvinylpyrrolidone, benzamidine, 2-mercaptoethanol, EDTA, bovine serum albumin, and Fura-2 were purchased from Sigma. Sephadex G-100 was purchased from Amersham Pharmacia Biotech. Bis-ANS was from Molecular Probes. Prestained SDS-PAGE standards were purchased from Bio-Rad. Polyvinylidene difluoride membrane was from PerkinElmer Life Sciences. All other reagents were of analytical grade. Mung bean (*V. radiata*) seeds were purchased from seed multiplication farm, Behrampur, West Bengal, India.

Two batches of [^{3}H]$Ins(1,4,5)P_3$ (specific activity, 0.677 and 21 μCi/nmol, respectively) and one batch of [^{3}H]$InsP_6$ (specific activity, 20.5 μCi/nmol) were obtained from PerkinElmer Life Sciences. [^{32}P]Orthophosphoric acid (specific activity, 6000 Ci/mmol) was obtained from BRIT, India. [^{32}P]$InsP_6$ was obtained from the precursor, [^{32}P]orthophosphoric acid, by a method reported earlier (9). In brief, the method consists of ion-exchange-based fractionation of *myo*-inositol phosphates from the mung bean seeds germinating for 48 h in [^{32}P]orthophosphoric acid-enriched medium. Concentration of purified $InsP_6$ was evaluated by estimation of phosphate liberated from $InsP_6$ after its complete digestion of $InsP_6$ with perchloric acid for 3 h at 180 °C (10). Specific activity of stock [^{32}P]$InsP_6$ was 248 cpm/pmol.

Isolation of Phytase—Phytase was isolated from cotyledons of 72-h germinating seeds by the modified method of Mandal and co-workers (2, 3). The preparation was tested for phytase activity from estimation of liberated phosphate from the substrate, $InsP_6$, at 37 °C. Purity of the protein was confirmed by means of SDS-PAGE from the presence of a single band of 160 kDa. Contamination of nonspecific phosphatase in the purified enzyme was not detected because the preparation does not hydrolyze glucose 6-phosphate, which is a substrate for phosphatase (3). For fluorescence spectroscopic studies, the protein, which was eluted from the 5% non-denaturing gel, was passed through Sephadex G-75 (Superfine) to remove possible fluorescent contaminants from the gel. Its concentration was determined by the method of Lowry *et al.* (11) or by the Bradford assay (12).

Limited Proteolysis of Phytase by Trypsin—Trypsin, insoluble enzyme attached to beaded agarose (from Bovine Pancreas, suspended in ~10 mM acetic acid, pH 3.2), was washed repeatedly with excess of 50 mM Tris-HCl buffer, pH 7.0. Phytase (75 μg) was incubated with 4 units of trypsin in the 50 mM Tris-HCl buffer, pH 7.0, containing 50 mM NaCl for 3 h at 30 °C. Trypsin was removed from the incubation mixture by centrifugation at 4,000 × *g* for 5 min. A 7.5% SDS-PAGE was done to characterize the fragments of trypsinized phytase. Size-exclusion chromatography of the trypsinized phytase was carried out to isolate the tryptic fragments for further experiments. Trypsinized phytase (after removal of trypsin) was loaded onto Sephadex G-100 column (0.5 × 30.0 cm). The tryptic fragments were eluted from the column with 50 mM Tris-HCl buffer, pH 7.0, at an elution rate of 0.1 ml/min. Fractions were monitored using fluorescence intensity at 340 nm (λ_{ex} = 278 nm, where λ_{ex} indicates excitation wavelength). Peak fractions were pooled and concentrated. Concentration of the fragments was determined using the method of Lowry *et al*. (11) or by the Bradford assay (12).

Assay of Phytase Activity—Assay of enzyme activity for phytase and its tryptic fragments is based on the estimation of inorganic phosphate liberated from the phytase-catalyzed dephosphorylation of the substrate, $InsP_6$. In all assays, the concentration of phytase/its tryptic fragment(s) was 625 nM, whereas that of $InsP_6$ was 2 mM. During the assay with native enzyme, it was incubated with $InsP_6$ for 1 h at 37 °C in 50 mM Tris-HCl buffer, pH 7.5. In experiments to check the effect of the high affinity site upon the catalytic potential of phytase, the site was first saturated by preincubation of phytase either with 300 nM $Ins(1,4,5)P_3$/$Ins(2,4,5)P_3$ or 500 nM $Ins(1,3,4)P_3$ in 50 mM Tris-HCl buffer, pH 7.5, at 4 °C for 15 min followed by the routine assay procedure. Inorganic phosphate liberated was estimated by the ascorbate method (13) or by the method of continuous fluorimetry (14). The method of continuous fluorimetry was employed during the early phase of catalysis (1–5 min) when the amount of phosphate liberated from the substrate was too low to be detected by the ascorbate method. In this method, phosphate released from $InsP_6$ hydrolysis is coupled to the nucleoside phosphorylase reaction using 7-methylguanosine as a fluorescent substrate (14). In either of the above methods inorganic phosphate was quantitated from the calibration curve using standards in the same range of concentrations as that liberated from $InsP_6$ by phytase.

For enzyme kinetics under different conditions, phytase was incubated with $InsP_6$ in 50 mM Tris-HCl buffer, pH 7.5, at 37 °C for various time intervals, and the phosphate liberated was quantitated as explained above. The kinetics of enzyme activity is expressed in units of phosphate (μmol) liberated per h per mg of protein at 37 °C (2, 15, 16).

Reconstitution Assay—In all reconstitution studies the tryptic fragments were mixed at equimolar ratio in 50 mM Tris-HCl buffer, pH 7.5, and incubated for 15 min at 4 °C. Reconstituted mixture was assayed for phytase activity as mentioned above using $InsP_6$ as the substrate.

Fluorescence Spectroscopic Studies—All fluorescence spectra were recorded in Shimadzu RF-540 spectrofluorometer using an excitation wavelength of 278 nm (excitation slit width = 5 nm and emission slit width = 10 nm). The steady value of fluorescence emission at 340 nm with time indicated the absence of any potential photodegradation of the enzyme. All dissociation constants were evaluated in 50 mM Tris-HCl buffer, pH 7.0, at different temperatures. In general temperatures were kept at or below 15 °C to avoid enzymatic cleavage of the substrate, $InsP_6$ (3). During fluorescence titration, aliquots of the corresponding *myo*-inositol phosphate were added to a fixed concentration of phytase/tryptic fragment(s). Fluorescence emission spectra of the protein (λ_{em} = 300-450 nm and λ_{ex} = 278 nm where λ_{em} indicates fluorescence emission wavelength) were monitored as a function of the input concentrations of ligand.

During evaluation of the dissociation constant of phytase (or its tryptic fragment)-$InsP_6$ interaction in the presence of $InsP_3$, the enzyme was preincubated with 300 nM $Ins(1,4,5)$/$(2,4,5)P_3$ or 500 nM $Ins(1,3,4)P_3$ for 15 min at the experimental temperature, and then aliquots of $InsP_6$ were added.

Dissociation constant (K_d) for protein-substrate interaction was determined by means of nonlinear curve fitting of the experimental points based on the following equilibrium: L + P ⇔ L − P; where L and P denote the ligand and protein, respectively. Curve fitting was done according to Equations 1 and 2. Goodness of the fit was ascertained by least square analysis.

$$K_d = (C_p - (\Delta F/\Delta F_{max})C_p)\,(C_l - (\Delta F/\Delta F_{max})C_p)/((\Delta F/\Delta F_{max})C_p) \quad \text{(Eq. 1)}$$

$$C_p(\Delta F/\Delta F_{max})^2 - (C_p + C_l + K_d)\,(\Delta F/\Delta F_{max}) + C_l = 0 \quad \text{(Eq. 2)}$$

where ΔF is the change in fluorescence emission intensity at 340 nm after addition of each aliquot of the ligand to the protein; ΔF_{max} is the same parameter when the protein is totally bound to the ligand; C_l is the input concentration of the ligand; and C_p, the initial concentration of the protein. Double-reciprocal plot ($1/\Delta F$ *versus* $1/C_l$, 17) was used for determination of ΔF_{max} using Equation 3,

$$1/\Delta F = 1/\Delta F_{max} + K_d/(\Delta F_{max}(C_l)) \quad \text{(Eq. 3)}$$

As stated in a previous report (3), hydrolysis of $InsP_6$ by phytase in the absence and presence of $InsP_3$ is found to be insignificant at the experimental temperatures.

Fluorescence quenching experiments were carried out by recording fluorescence intensities at 340 nm (λ_{ex} = 295 nm). Aliquots from a stock solution of a neutral quencher acrylamide were added successively to phytase (0.3 μM) preincubated with 300 nM $Ins(1,4,5)P_3$ and 2 mM $InsP_6$ for 15 min at 4 °C in 50 mM Tris-HCl buffer, pH 7.0. Quenching data were analyzed according to the Stern-Volmer equation (18), $F_o/F = 1 + K_{sv}[Q]$, where F_o and F are the initial and final fluorescence intensities, respectively. K_{sv} is the quenching constant, and $[Q]$ denotes the input concentration of acrylamide. A modified Stern-Volmer plot (19) was also done to estimate the accessible (f_e) fraction of tryptophan residues according to Equation 4,

$$F_o/(F_o - F) = 1/(K_{sv}\,f_e[Q]) + 1/f_e \quad \text{(Eq. 4)}$$

For fluorescence studies with bis-ANS, it was dissolved in freshly distilled dimethyl sulfoxide. The concentration of the solution was determined from ϵ_{396} = 24,300 M^{-1} cm^{-1}. All fluorescence emission spectra (λ_{em} = 420–600 nm, λ_{ex} = 399 nm) were recorded in 50 mM Tris-HCl buffer, pH 7.0, at 15 °C in a Shimadzu RF-540 spectrofluorometer. Fluorimetric titrations were done by adding aliquots of bis-ANS to a fixed concentration of phytase (0.3 μM) under different conditions. The fluorescence value at 484 nm was recorded after it became steady. The value was corrected for fluorescence of bis-ANS alone in buffer and contribution of the buffer, if any.

Filter Binding Assay—In general, radiolabeled $InsP_6$/$Ins(1,4,5)P_3$ was incubated with a fixed concentration of phytase or its tryptic fragment. The mixture was incubated under appropriate conditions of buffer and temperature. The temperature was kept low to avoid possible hydrolysis of the substrate by the enzyme (or its tryptic fragment). The incubation mixture was spotted onto Whatman GF/C filter paper, washed with the same buffer, dried, and counted. Nonspecific binding

was checked in the presence of 10-fold excess of non-radioactive $InsP_6$/Ins(1,4,5)P_3.

For evaluation of dissociation constant for phytase-$InsP_6$ interaction, different concentrations of [^{3}H]$InsP_6$ (specific activity, 2288 cpm/nmol) were incubated with phytase in 50 mM Tris-HCl buffer, pH 7.0, at 10 °C for 45 min. Specifically bound count was plotted as a function of input concentrations of $InsP_6$ to construct the binding isotherm. The dissociation constant was calculated from the concentration of $InsP_6$ corresponding to half of the bound counts/min.

Binding of $InsP_6$ to phytase was also checked after phytase was preincubated with $InsP_3$. Phytase and Ins(1,4,5)/(2,4,5)P_3 (300 nM) or Ins(1,3,4)P_3 (500 nM) were incubated in 50 mM Tris-HCl buffer, pH 7.0, for 15 min at 4 °C. [^{3}H]$InsP_6$ (specific activity, 2288 cpm/nmol) was added to a final concentration of 20 μM. The normal filter binding assay was conducted, and specifically bound counts were determined.

To determine stoichiometry of binding, phytase or its tryptic fragment was incubated with [^{32}P]$InsP_6$ (specific activity, 248 cpm/pmol) or [^{3}H]Ins(1,4,5)P_3 (specific activity, 110 cpm/pmol) in 50 mM Tris-HCl buffer, pH 8.0, at 4 °C. Moles of ligand bound were calculated from specifically bound counts (from the filter binding assay). The quotient of the ligand bound and input concentration of protein used gave the stoichiometry "*n*."

Dissociation constant for phytase or its tryptic fragment-Ins(1,4,5)P_3 interaction at the high affinity site was determined by filter binding assay using [^{3}H]Ins(1,4,5)P_3 after incubating the components in 50 mM Tris-HCl buffer, pH 8.0, at 10 °C for 1 h. The dissociation constant was calculated from the binding isotherm as explained above.

Evaluation of Thermodynamic Parameters—Free energy of the interaction, ΔG, was evaluated (20), using Equation 5,

$$\Delta G = -RT \ln K_a \quad \text{(Eq. 5)}$$

where the association constant

$$K_a = 1/K_d \quad \text{(Eq. 6)}$$

K_a determined at three different temperatures was used for calculation of the thermodynamic parameters. Changes in enthalpy [ΔH] and entropy [ΔS] were evaluated from van't Hoff plots of $\ln K_a$ against $1/T$ according to the Equations 6 and 7,

$$\ln K_a = -\Delta H/RT + \Delta S/R \quad \text{(Eq. 7)}$$

where R and T are universal gas constant and absolute temperature, respectively (10).

Preparation of Microsomes/Vacuoles and Assay of Ca^{2+} Release—Microsomes/vacuoles were prepared as reported earlier (3). Hypocotyls from 48-h germinating mung bean seeds were homogenized in buffer A containing 25 mM Tris-HCl buffer, pH 8.0, 0.25 M sucrose, 3 mM EDTA, 10 mM 2-mercaptoethanol, 1 mM phenylmethylsulfonyl fluoride, 1 mM benzamidine, 1 g/liter bovine serum albumin, and 10 g/liter polyvinylpyrrolidone. The homogenate was passed through two layers of cheesecloth. It was then centrifuged at 12,000 × *g* for 40 min, and the supernatant was finally centrifuged at 80,000 × *g* for 1 h at 4 °C to pellet the microsomes/vacuoles. This pellet was resuspended in buffer B containing 50 mM Tris-HCl buffer, pH 8.0, 0.25 M sucrose, 100 mM KCl, 2 mM $MgCl_2$ for Ca^{2+} uptake and release experiments. The concentration of the protein in the microsomal/vacuolar suspension was determined by the method of Lowry *et al*. (11).

Concentration of calcium was evaluated by using Ca^{2+} indicator fluorescent dye Fura-2 (λ_{em} = 510 nm and λ_{ex} = 340 nm) in a Shimadzu RF-540 spectrofluorometer. For the evaluation of Ca^{2+} influx and efflux, microsomal/vacuolar suspension (260 μg/ml) in buffer (containing 50 mM Tris-HCl buffer, pH 8.0, 0.25 M sucrose, 100 mM KCl, 2 mM $MgCl_2$) was incubated at 20 °C with 3 mM NaN_3 to prevent any mitochondrial uptake, Fura-2 (1 μM), and $CaCl_2$ (100 μM). ATP was added to a final concentration of 2 mM to initiate the uptake of Ca^{2+} by the microsomes/vacuoles. Uptake was monitored from the decrease in fluorescence of Fura-2. After the process of uptake had reached equilibrium as indicated from absence of any fluorescence change, Ins(1,4,5)P_3 or Ins(1,4,5)P_3 complex with phytase/tryptic fragment(s) of phytase/equimolar mixture of two relevant tryptic fragments was added to stimulate Ca^{2+} release. Calcium release was followed over a period of 20 s.

Concentration of released Ca^{2+} was calculated from the following Equation 8 (21),

$$[Ca^{2+}] = K_d(F - F_{min})/(F_{max} - F) \quad \text{(Eq. 8)}$$

where K_d (dissociation constant for Fura-2-Ca^{2+} interaction) = 135 nM (22), F_{max}, the maximum fluorescence of Fura-2 in presence of 2 mM $CaCl_2$ and F_{min}, the minimum fluorescence of Fura-2 in the presence of 5 mM EGTA. F is the fluorescence of Fura-2 upon addition of ATP or Ca^{2+}-mobilizing agents.

Amino Acid Sequencing and Homology Searching—Concentrated 5-kDa tryptic fragment was electrophoresed on a 20% SDS-PAGE. Following electrophoresis, protein was blotted onto a polyvinylidene difluoride membrane, and an automated protein sequenator (PerkinElmer Life Sciences) was used to sequence about 12 amino acids from the N-terminal end. Homology search for the amino acid sequence was carried out using the Fasta-3 program (23) with SWALL and SPTrEMBL as data bases (www.ebi.ac.uk). The upper expectation value (E value) was set at 1.0, and the lower expectation value was $1 \times e^{-6}$. Search for structural homology was carried out using CATH program (24) and FSSP search program (25).

RESULTS

Evaluation of Dissociation Constant of Phytase-$InsP_6$ Interaction and Effect of Nanomolar Concentrations of $InsP_3$ upon Association of Phytase and $InsP_6$—We have demonstrated previously (3) association of the substrate, $InsP_6$, with phytase from a decrease in the quantum yield of protein fluorescence upon addition of the substrate, and we determined the dissociation constant for the phytase-$InsP_6$ interaction. Here we have further verified the value by filter binding assay employing radiolabeled $InsP_6$. Binding isotherms from both methods are shown in Fig. 1, *a* and *b*. In the fluorescence method, dissociation constant determined from the curve fitting procedure is 33 μM at 10 °C. The corresponding value that was determined from filter binding assay at the same temperature is 38 μM, thereby supporting the validity of the application of fluorescence method.

Dissociation constant for phytase-Ins(1,4,5)P_3 association at the non-catalytic site is 75 nM. The same value at the catalytic site is 3 μM (3). Therefore, we have chosen a concentration of 300 nM Ins(1,4,5)P_3/Ins(2,4,5)P_3 to ensure that the high affinity binding site in phytase is selectively saturated. However, as higher concentration of Ins(1,3,4)P_3 was required to saturate the high affinity site (3), we used 500 nM Ins(1,3,4)P_3 to saturate selectively the high affinity site. Hydrolysis of $InsP_3$ by phytase does not occur at these concentrations of $InsP_3$.

Pre-association of anyone of the three *myo*-inositol trisphosphates with phytase at the high affinity site did not change the fluorescence spectrum of phytase significantly. Fig. 2, *a* and *b*, shows the change in fluorescence spectra of phytase, preincubated with Ins(1,4,5)P_3/Ins(2,4,5)P_3, after addition of $InsP_6$ at 10 °C. The presence of an isosemmitic point around 440 nm in both sets suggests formation of a single type of complex even after saturation of the high affinity site. A titration profile was obtained from the concentration-dependent decrease in the fluorescence of phytase. Dissociation constants were calculated from such profiles using nonlinear curve fitting analysis. Representative curves are shown in Fig. 3. A summary of the results is given in Table I. Results in the table show that presaturation of the high affinity site with 300 nM Ins(1,4,5)P_3/Ins(2,4,5)P_3 or with 500 nM Ins(1,3,4)P_3 increases the affinity of phytase for $InsP_6$.

Increase in the affinity of phytase for $InsP_6$ as a result of the pre-saturation with either of the three isomers Ins(1,4,5)/(2,4,5)/(1,3,4)P_3 at the non-catalytic site is also indicated from the results shown in Table II. In all cases preincubation with Ins(1,4,5)/(2,4,5)/(1,3,4)P_3 leads to an increase in the bound $InsP_6$. It further substantiates the conclusion from fluorescence spectroscopic study.

In a reverse approach we have checked under the same conditions the binding efficiency of phytase at the high affinity site for Ins(1,4,5)P_3 when the enzyme has $InsP_6$ at the catalytic site. There is an enhancement as indicated from the increase in number of specifically bound counts of [^{3}H]Ins(1,4,5)P_3 (249 ±

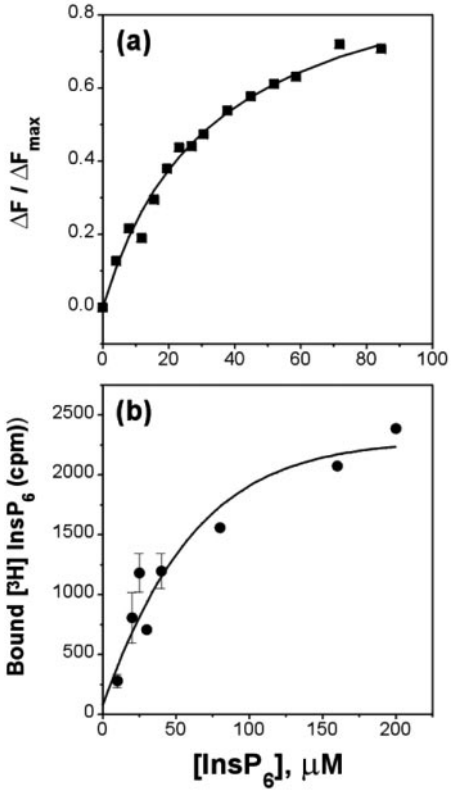

FIG. 1. **Interaction of $InsP_6$ with phytase in 50 mM Tris-HCl buffer, pH 7.0, at 10 °C.** Binding isotherms for the interaction of $InsP_6$ with phytase by spectrofluorometric titration (■) (*a*) and by filter binding assay using [^{3}H]$InsP_6$ (●) (*b*). During spectrofluorometric titration, aliquots of $InsP_6$ were added to phytase (0.3 μM) in 50 mM Tris-HCl buffer, pH 7.0, at 10 °C. From such titrations $\Delta F/\Delta F_{max}$ was calculated as follows. $\Delta F = F_o - F$, where F_o and F are the fluorescence emission intensities of phytase at 340 nm (λ_{ex} = 278 nm) alone and after each addition of each aliquot of $InsP_6$, respectively. ΔF_{max} was obtained from the reciprocal of the intercept in the plot of $1/\Delta F$ against $1/C_l$. Nonlinear fitting of experimental points, as explained under "Experimental Procedures," generated the theoretical curve. Binding of [^{3}H]$InsP_6$ to phytase was monitored by filter binding assay as explained under "Experimental Procedures." Representative *error bars* shown in the figures are obtained from three different sets of experiments. Dissociation constant is calculated from the concentration of $InsP_6$ corresponding to half of the bound counts/min.

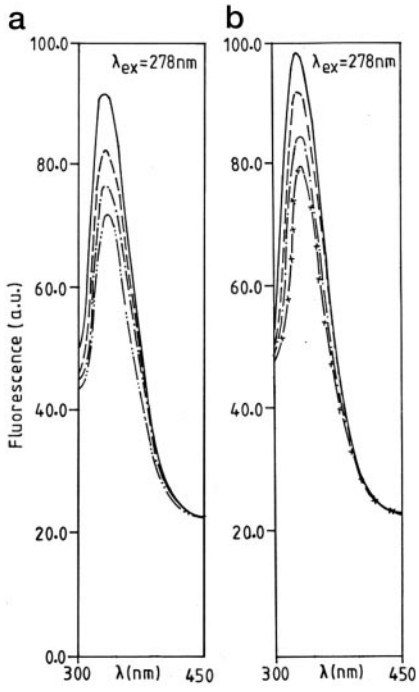

FIG. 2. **Fluorescence emission spectra (λ_{ex} = 278 nm) of phytase (0.3 μM) under different conditions in 50 mM Tris-HCl buffer, pH 7.0, at 10 °C.** *a,* preincubated with $Ins(1,4,5)P_3$ (300 nM, —) and in the presence of $InsP_6$ (2.3 μM, – – –; 29.6 μM, —·—; and 35.2 μM, –··–). *b,* preincubated with $Ins(2,4,5)P_3$ (300 nM, —) and in the presence of $InsP_6$ (0.3 μM, – – –; 4.3 μM, —·—; and 9.2 μM, –×–).

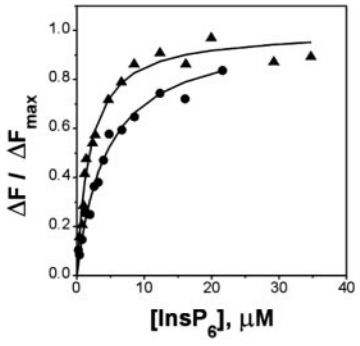

FIG. 3. **Binding of $InsP_6$ to phytase preincubated with *myo*-inositol trisphosphates in 50 mM Tris-HCl buffer, pH 7.0, at 10 °C.** Binding isotherms for the interaction of $InsP_6$ with phytase (0.3 μM) after preincubation with $Ins(1,4,5)P_3$, (300 nM, ▲), and $Ins(2,4,5)P_3$, (300 nM, ●) were constructed from spectrofluorometric titrations as explained under "Experimental Procedures" by means of nonlinear curve fitting analysis.

50 cpm) in comparison to that for the native enzyme (138 ± 20 cpm). It suggests that the interaction between the two sites is mutual.

The comparison of binding affinity at a single temperature may not provide the complete picture; therefore, we evaluated the energetics of the association between phytase and $InsP_6$ under the conditions mentioned in Table III. Representative van't Hoff plots are shown in Fig. 4. Table III lists the thermodynamic parameters. It shows an alteration in their values when phytase is saturated at the high affinity site, although the entropy-driven nature of the phytase-$InsP_6$ association remains unaltered. Another notable feature is the extent of change in enthalpy and entropy; it follows a decreasing order: $Ins(1,4,5)P_3 < Ins(2,4,5)P_3 < Ins(1,3,4)P_3$. First among the three is the most potent second messenger, $Ins(1,4,5)P_3$.

Effect of Presence of Saturating Concentrations of myo-Inositol Trisphosphates at the High Affinity Site on the Kinetics of the Hydrolysis of $InsP_6$ by Phytase—The stabilizing effect of the presence of $Ins(1,4,5)P_3$/$Ins(2,4,5)P_3$ at the high affinity site upon phytase-$InsP_6$ association was further probed in the following way. By employing $InsP_6$ as the substrate, we measured the dephosphorylating activity of phytase after presaturation with the above trisphosphates. The boosting effect of the three *myo*-inositol trisphosphate isomers upon the catalytic activity of phytase corresponding to a single time point is summarized in Table IV. In all cases, there is a significant increase in the enzymatic activity as a sequel to presaturation of the high affinity site. The extent of increase is dependent upon the isomeric nature of the trisphosphate, thereby supporting the view that it is a specific effect. Since $Ins(1,4,5)P_3$ is well established as a second messenger (4, 6) and $Ins(2,4,5)P_3$ is one of the sequential dephosphorylation products from $InsP_6$ in *V. radiata* (26), we made a detailed comparison of the effect of their binding upon the kinetics of dephosphorylation of $InsP_6$ by phytase. Fig. 5 shows the kinetics of phytase activity, in the presence and absence of 300 nM $Ins(1,4,5)P_3$/$Ins(2,4,5)P_3$. The *inset* to Fig. 5 contains the values of phosphate liberated corresponding to the early time points ranging between one and five min. Phosphate liberated at 5 min after incubation of $InsP_6$ was estimated by both methods. The values are self-consistent,

TABLE I

Effect of myo-inositol trisphosphates on phytase-InsP_6 interaction

K_d for phytase-InsP_6 interaction under different conditions in 50 mM Tris-HCl buffer, pH 7.0, at 10 °C was estimated using a variation of the method reported earlier (3). In brief, aliquots of InsP_6 were added to phytase (0.3 μM) alone or preincubated with InsP_3 for 15 min at the experimental temperature. Fluorescence emission intensity of protein was recorded at 340 nm (λ_{ex} = 278 nm) after it reached a steady value following each addition. Dissociation constants were calculated from the spectrofluorometric titrations using a method of nonlinear curve fit that is explained under "Experimental Procedures." Typical standard deviations in dissociation constant values are 20%.

System	K_d
	μM
Phytase	33
Phytase preincubated with Ins(1,4,5)P_3 (300 nM)	1.7
Phytase preincubated with Ins(2,4,5)P_3 (300 nM)	4.0
Phytase preincubated with Ins(1,3,4)P_3 (500 nM)	5.2

TABLE II

Effect of preincubation of phytase with Ins(1,4,5)/(2,4,5)/(1,3,4)P_3 at the high affinity site upon binding of [^{3}H]InsP_6 to the enzyme

Phytase (0.4 μM) was incubated with Ins(1,4,5)/(2,4,5)P_3 (300 nM) or Ins(1,3,4)P_3 (500 nM) in 50 mM Tris-HCl buffer, pH 7.0, at 4 °C for 15 min. [^{3}H]InsP_6 (specific activity = 2288 cpm/nmol) was added to the mixture so that the final concentration of InsP_6 was 20 μM. The mixture was incubated for 45 min at 10 °C followed by filter binding assay. The data below represent the mean of two sets of experiments.

System	Counts/min [^{3}H]InsP_6 specifically bound
Phytase alone	780 ± 65
Phytase preincubated with Ins(1,4,5)P_3 (300 nM)	1280 ± 50
Phytase preincubated with Ins(2,4,5)P_3 (300 nM)	1110 ± 86
Phytase preincubated with Ins(1,3,4)P_3 (500 nM)	1060 ± 31

TABLE III

Effect of preincubation of phytase with Ins(1,4,5)/(2,4,5)/(1,3,4)P_3 upon the thermodynamic parameters for phytase-InsP_6 interaction

Saturation of the high affinity site in phytase (0.3 μM) was done by incubating any of the three *myo*-inositol trisphosphates at the concentration indicated below with phytase for 15 min at the experimental temperature in 50 mM Tris-HCl buffer, pH 7.0. The dissociation constant for each system was measured at 5, 10, and 15 °C. Free energy, ΔG, at 10 °C is calculated from Equation 5. Enthalpy change, ΔH, and entropy change, ΔS, were evaluated from van't Hoff plot of lnK_a versus 1/T (Equations 6 and 7). The data below represent mean of two sets of experiments.

System	Thermodynamic parameters		
	ΔG	ΔH	ΔS
	kcal/mol		*e.u.*
Phytase alone	−5.8	+14.6	+71.9
Phytase preincubated with Ins(1,4,5)P_3 (300 nM)	−7.4	+9.0	+58.0
Phytase preincubated with Ins(2,4,5)P_3 (300 nM)	−7.0	+12.0	+67.1
Phytase preincubated with Ins(1,3,4)P_3 (500 nM)	−6.8	+15.3	+77.9

thereby supporting the methods of estimation for phosphate. It is evident that the presence of the *myo*-inositol trisphosphates enhances the rate of dephosphorylation of InsP_6 by phytase, the extent of increase in the rate being more pronounced in case of Ins(1,4,5)P_3. Dephosphorylation curves in the presence of Ins(1,4,5)P_3 and Ins(2,4,5)P_3 differ in the values of the slope. This is particularly true for the initial lag phase.

Limited Proteolysis of Phytase—Previously reported results (3) and the data presented above clearly support the bifunctional nature of phytase. We proceeded to trypsinize phytase with a view to checking whether the two functions originate from two different sites, and if so, whether there is an interaction between the sites contained in two separate peptide fragments.

Gel elution profile of trypsinized phytase shows six peaks (Fig. 6*a*). Peak positions were detected by intrinsic fluorescence

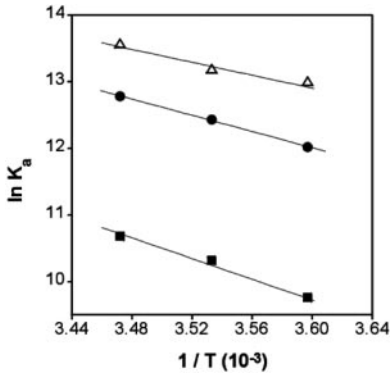

FIG. 4. **van't Hoff plots for phytase-InsP_6 interaction in 50 mM Tris-HCl buffer, pH 7.0, under different conditions.** Phytase alone (-■-), after preincubation of phytase with 300 nM Ins(1,4,5)P_3 (-△-), and 300 nM Ins(2,4,5)P_3 (-●-). Best fit lines were drawn using least square analysis.

TABLE IV

Effect of preincubation of phytase with Ins(1,4,5)/(2,4,5)/(1,3,4)P_3 upon dephosphorylation of InsP_6 by the enzyme

Phytase, alone or presaturated with InsP_3, was incubated with 2 mM InsP_6 for 45 min at 37 °C in 50 mM Tris-HCl buffer, pH 7.5. Enzymatic activity was quantitated from an estimation of the liberated inorganic phosphate using ascorbate method, given under "Experimental Procedures." Concentrations of the various components are indicated in parentheses.

System	Phosphate liberated
	μmol/h/mg protein
Phytase alone (625 nM)	93.8 ± 2.1
Phytase (625 nM) preincubated with Ins(1,4,5)P_3 (300 nM)	154.6 ± 2.1
Phytase (625 nM) preincubated with Ins(2,4,5)P_3 (300 nM)	160.0 ± 4.3
Phytase (625 nM) preincubated with Ins(1,3,4)P_3 (500 nM)	138.6 ± 5.3

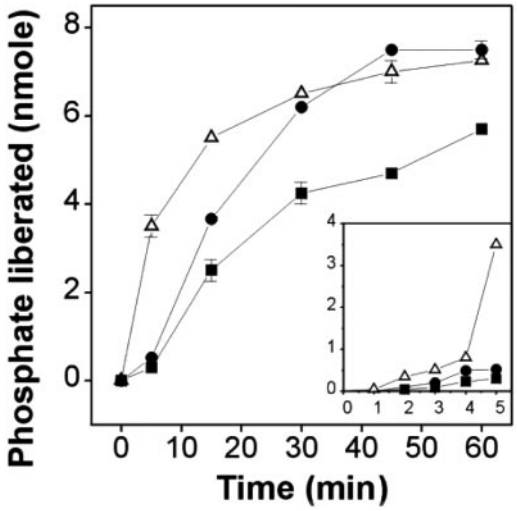

FIG. 5. **Kinetics of dephosphorylation of InsP_6 by phytase under different conditions in 50 mM Tris-HCl buffer, pH 7.5, at 37 °C.** Phytase alone (-■-), phytase preincubated with 300 nM Ins(1,4,5)P_3 (-△-), and phytase preincubated with 300 nM Ins(2,4,5)P_3 (-●-). *Inset* shows kinetics of phytase catalyzed dephosphorylation of InsP_6 in the first 5 min by phytase alone (-■-), in the presence of 300 nM Ins(1,4,5)P_3 (-△-), and in the presence of 300 nM Ins(2,4,5)P_3 (-●-). Representative *error bars* shown in the figure are obtained from three different sets of experiments.

of the peptides. Peaks II–V correspond to trypsinized fragments of 66, 33, 22.5, and 5 kDa, respectively. Molecular weights were determined from a standard calibration curve of molecular weight against elution volume (Fig. 6*b*). Peak I ap-

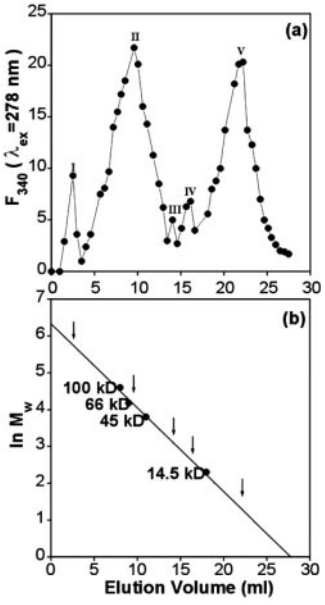

FIG. 6. **Isolation and characterization of molecular masses of the tryptic fragments of phytase by gel filtration through Sephadex G-100.** *a,* 75 μg of trypsinized phytase in the 150 μl of 50 mM Tris-HCl buffer, pH 7.0, plus 50 mM NaCl was loaded onto the column. 50 mM Tris-HCl buffer, pH 7.0, was the elution buffer. The size of each fraction was 0.5 ml. Fluorescence (340 nm, λ_{ex} = 278 nm) for each fraction was plotted against the elution volume. *b,* standard proteins were T7RNA polymerase (100 kDa), bovine serum albumin (66 kDa), ovalbumin (45 kDa), and lysozyme (14.5 kDa). *Arrows* indicate the positions of elution of the tryptic fragments of phytase. *Peaks II* and *V* correspond to 66- and 5-kDa fragments, respectively.

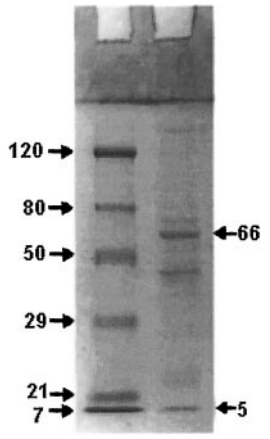

FIG. 7. **SDS-PAGE of trypsinized phytase.** *Right lane,* prestained marker; *left lane,* trypsinized protein, 17 μg. Molecular size of marker proteins are shown on the *left* and molecular masses of two major tryptic fragments are indicated on the *right.* Gels were stained with Coomassie Brilliant Blue R-250.

TABLE V
Stoichiometry for association of $InsP_6$ or Ins(1,4,5)P_3 with phytase or its tryptic fragments

Phytase or its tryptic fragment (100 nM) was incubated with [^{32}P]$InsP_6$ (100 μM, specific activity = 248 cpm/pmol) in 50 μl of 50 mM Tris-HCl buffer, pH 8.0, at 4 °C for 15 min. Similarly, [^{3}H]Ins(1,4,5)P_3 (300 nM, specific activity = 110 cpm/pmol) was incubated with phytase or its tryptic fragment (100 nM) in 60 μl of 50 mM Tris-HCl buffer, pH 8.0, at 4 °C for 15 min. Filter binding assay was then carried out as described under "Experimental Procedures." The data below represent mean of two sets of experiments with S.D. of 10%.

Protein	Counts/min [^{32}P]$InsP_6$ specifically bound	*n*	Counts/min [^{3}H]$InsP_3$ specifically bound	*n*
Phytase	1118	0.9	715	1.1
66-kDa fragment	1154	0.9	150	0.2
5-kDa fragment	40	0.03	577	0.9

pearing to the *left* of *peak II* (Fig. 6*a*) in the void volume of the column, corresponds to the undigested, native phytase (160 kDa). This was also evident from the coinciding peak position in the elution profile of the native enzyme passed through the column in a separate experiment.

The number of trypsinized fragments was also confirmed by SDS-PAGE (Fig. 7). It shows the presence of six bands including the undigested phytase. There is an apparent discrepancy between the number of fragments obtained by both methods. It may be due to the fact that some fragments do not have quantum yield high enough for detection by fluorescence.

Characterization of the Tryptic Fragments of Phytase in Terms of $InsP_6$ Binding and High Affinity Ins(1,4,5)P_3 Binding Potentials—Each tryptic fragment from gel elution was tested for $InsP_6$ binding using [^{32}P]$InsP_6$. $InsP_6$ binding ability was found only with 66-kDa fragment (Table V). By having established that the 66-kDa fragment binds $InsP_6$, we tested all fragments for the high affinity $InsP_3$ binding. Only the 5-kDa fragment binds Ins(1,4,5)P_3. The 5-kDa fragment, however, exhibits only negligible binding to $InsP_6$. Similarly, the 66-kDa fragment does not exhibit any high affinity binding potential for $InsP_3$. Stoichiometry of $InsP_6$ and Ins(1,4,5)P_3 binding is found to be one ligand molecule per protein molecule or per molecule of 66- and 5-kDa fragment (Table V). These results establish that the associations indicated from the filter binding assay are specific in nature.

The above experiments have shown that the binding sites of phytase for the substrate and inositol trisphosphate(s) are located in two peptide fragments, 66 and 5 kDa, respectively. Therefore, we examined whether the fragments retain the functional features of the native protein.

Assay for the Enzymatic and Ca^{2+} Mobilization Activities of the Tryptic Fragments—We have compared the dephosphorylation potentials of 66- and 5-kDa fragments under different conditions with a view to examining their functions. We have also scrutinized whether the aforementioned rate-enhancing effect of trisphosphates upon the kinetics of dephosphorylation is observed with the 66-kDa fragment alone (negative control) and under the conditions where a truncated phytase has been reconstituted from 66- and 5-kDa fragments. The results are summarized in Table VI. The 66-kDa fragment shows dephosphorylation activity less than that of the native enzyme. Addition of the 5-kDa fragment leading to reconstitution of the enzyme restores about 75% of the native phytase activity. The presence of 300 nM Ins(1,4,5)P_3 does not cause any significant change in the dephosphorylation capability of 66-kDa fragment. On the other hand, reconstitution of the 66- and 5-kDa fragments in the presence of 300 nM $InsP_3$ increases the catalytic potential of the 66 kDa. These results support the idea that the dual functions of the enzyme could be ascribed to the sites present in the two fragments.

As reported earlier, high affinity binding of phytase with Ins(1,4,5)P_3 leads to enhanced mobilization of Ca^{2+} from intracellular stores such as vacuoles/microsomes (3, 27). Similar assays for calcium release from microsomes/vacuoles were carried with the two tryptic fragments of phytase. The fragments were preincubated with Ins(1,4,5)P_3, and their Ca^{2+} mobilization potentials were compared with the values obtained from Ins(1,4,5)P_3 alone. The results are summarized in Fig. 8. $InsP_3$-5-kDa fragment complex mobilizes Ca^{2+} from microsomes/vacuoles comparable to the phytase-Ins(1,4,5)P_3 high affinity complex and 3-fold more than that elicited by Ins(1,4,5)P_3 alone. On the other hand, Ins(1,4,5)P_3-66-kDa complex mobilizes calcium comparable to that released by Ins(1,4,5)P_3 alone. Reconstituted enzyme complexed with Ins(1,4,5)P_3 elicits cal-

TABLE VI
Dephosphorylation of $InsP_6$ by phytase or its tryptic fragments of phytase

66-kDa fragment or 5-kDa fragment was incubated with 2 mM $InsP_6$ for an hour at 37 °C in 50 mM Tris-HCl buffer, pH 7.5, and the inorganic phosphate liberated was quantitated using the ascorbate method (12). Concentrations of tryptic fragments and Ins(1,4,5)P_3 were 625 and 300 nM, respectively. Reconstitution of 66- and 5-kDa fragments was carried out as explained under "Experimental Procedures." Amount of phosphate liberated by phytase (625 nM) alone or after preincubation with 300 nM Ins(1,4,5)P_3 is included. The data below represent mean of two sets of experiments.

System	Phosphate liberated
	nmol
Phytase	5.9 ± 0.3
Phytase preincubated with Ins(1,4,5)P_3	7.25 ± 0.25
66-kDa fragment	2.5 ± 0.1
66-kDa fragment preincubated with Ins(1,4,5)P_3	2.3 ± 0.1
5-kDa fragment	0.9 ± 0.1
Reconstituted phytase (66-kDa fragment + 5-kDa fragment)	4.4 ± 0.1
Reconstituted phytase preincubated with Ins(1,4,5)P_3	6.5 ± 0.5

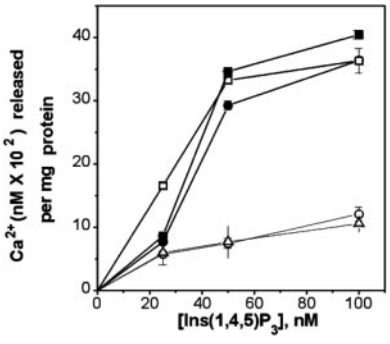

FIG. 8. **Intracellular Ca^{2+} release from microsomes/vacuoles.** Ins(1,4,5)P_3 alone (-○-), Ins(1,4,5)P_3-66-kDa fragment complex (-△-), Ins(1,4,5)P_3-5-kDa fragment complex (-●-), Ins(1,4,5)P_3-phytase complex (-■-), and Ins(1,4,5)P_3-reconstituted enzyme (66- + 5-kDa fragments) complex (-□-). The complex was made separately by incubating appropriate concentrations of $InsP_3$ and any one of the above for 15 min at 4 °C. 100 μl of the complex was added to a final volume of 1 ml of the microsomal/vacuolar suspension containing the remaining components. Ca^{2+} release was monitored over a period of 20 s, as explained under "Experimental Procedures." Each point shown is the mean obtained from two independent sets of experiments.

cium mobilization from microsomes/vacuoles comparable to the native enzyme.

Evaluation of Dissociation Constants and Thermodynamic Parameters for the 66-kDa Fragment-$InsP_6$ and the 5-kDa Fragment-Ins(1,4,5)P_3 Interactions—The above results clearly indicate the functional roles of the two tryptic fragments. Therefore, our next approach was to throw light on the molecular basis of interaction of $InsP_6$ and Ins(1,4,5)P_3 with the 66- and 5-kDa fragment, respectively. Knowledge of the energetics of association leads to a preliminary understanding of the basis of the interaction. Therefore, we evaluated the associated thermodynamic parameters. With this objective, K_d values were determined at three temperatures for 66-kDa-$InsP_6$ and 5-kDa-Ins(1,4,5)P_3 complexes.

As a control experiment we estimated the dissociation constant for the 66-kDa-$InsP_6$ interaction, after preincubation of the 66-kDa fragment with Ins(1,4,5)P_3. Binding isotherms obtained therefrom are shown in Fig. 9. Dissociation constants are 16.9 and 14.5 μM for the 66-kDa fragment-$InsP_6$ interaction in the absence and presence of $InsP_3$, respectively. Preincubation with Ins(1,4,5)P_3, however, does not affect the affinity of 66-kDa fragment for $InsP_6$.

Dissociation constant for phytase-Ins(1,4,5)P_3 complex evaluated by filter binding assay using [^{3}H]Ins(1,4,5)P_3 at 10 °C is 100 nM (Fig. 10). Thermodynamic parameters were determined from dissociation constants at 5 and 10 °C.

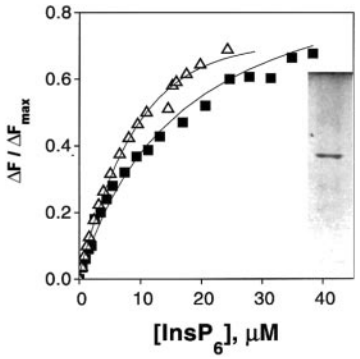

FIG. 9. **Binding analysis for 66-kDa fragment (0.3 μM)-$InsP_6$ association in 50 mM Tris-HCl buffer, pH 7.0, at 10 °C in absence of Ins(1,4,5)P_3 (■) and after preincubation with 300 nM Ins(1,4,5)P_3 (△).** Binding isotherms were generated from spectrofluorometric titrations using nonlinear curve fit analysis explained under "Experimental Procedures." *Inset* shows 66-kDa protein band on a 7.5% SDS-PAGE stained with Coomassie Brilliant Blue.

We have evaluated the dissociation constant for 5-kDa-Ins(1,4,5)P_3 interaction at 5 °C, by filter binding assay using [^{3}H]Ins(1,4,5)P_3 and fluorimetric titration as well at the same temperature. Fig. 11, *a* and *b,* shows the resultant binding isotherms. Dissociation constants, evaluated from filter binding assay and fluorimetry, are 75 and 52 nM, respectively.

Thermodynamic parameters (Table VII) for the above interactions indicate that interaction of $InsP_6$ with phytase or the 66-kDa fragment is entropy-driven; in contrast association of Ins(1,4,5)P_3 with phytase or 5-kDa fragment at the high affinity binding site is enthalpy-driven.

Conformational Probes of the Two Sites—Our previous report (3) has demonstrated that association of the substrate at the catalytic site of phytase results in a conformational change of the protein (f_e = 0.98 for free phytase and f_e = 0.65 for phytase saturated at the catalytic site with $InsP_6$). It also indicated that the high affinity association at the second site leads to a conformational change, which is a determinant for the association of phytase-Ins(1,4,5)P_3 complex with the receptor. The accessibility of tryptophan residues to acrylamide after phytase was saturated at the catalytic site followed by the high affinity site with $InsP_6$ and Ins(1,4,5)P_3, respectively, is 0.85.

We have also employed bis-ANS as the probe to monitor the difference, if any, in the nature of conformational changes of phytase when it binds to the substrate or *myo*-inositol trisphosphate. Results are shown in Fig. 12. The increase in fluorescence of bis-ANS upon association with native phytase results from the binding of the probe to hydrophobic pockets. The increase is not influenced to a significant degree when the catalytic site is saturated with $InsP_6$. In contrast, saturation of the high affinity site with Ins(1,4,5)P_3 reduces the fluorescence of bis-ANS to a marked extent. Control study of the effect of saturation of both sites upon the fluorescence of bis-ANS shows the same trend as mentioned above. Finally, these results clearly indicate that conformational changes that occur as a consequence of substrate binding and high affinity trisphosphate binding are different in nature. The latter one leads to a reduction in the available binding sites for a hydrophobic probe like bis-ANS.

Amino Acid Sequence and Homology Search—The first 12 amino acids from the N-terminal of the 5-kDa tryptic fragment are KRARTEYGRAAQ. The results of the homology search for this sequence are shown in Fig. 13*a*. The search results give an interesting observation that the sequence bears homology (75%

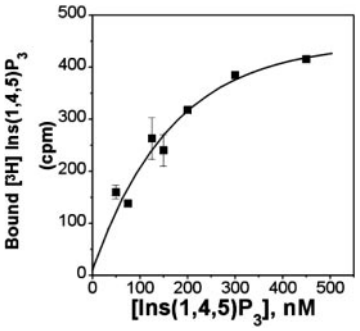

FIG. 10. **High affinity binding of Ins(1,4,5)P_3 to phytase in 50 mM Tris-HCl buffer, pH 8.0, at 10 °C.** Phytase (0.1 μM) was incubated with different concentrations of [^{3}H]Ins(1,4,5)P_3 (specific activity, 448 cpm/pmol). Specifically bound counts from the filter binding assay were plotted against concentration of Ins(1,4,5)P_3. Representative *error bars* shown in the figure are obtained from three different sets of experiments. Dissociation constant was calculated as the concentration of Ins(1,4,5)P_3 corresponding to the half of the bound counts.

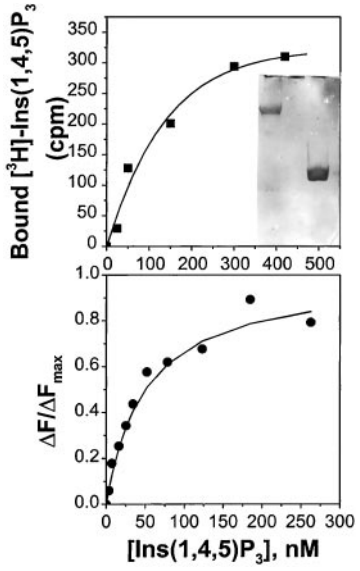

FIG. 11. **High affinity binding of Ins(1,4,5)P_3 to the 5-kDa fragment of phytase.** *a,* filter binding assay using [^{3}H]Ins(1,4,5)P_3 (■, specific activity, 163 cpm/pmol). Representative *error bars* shown in the figure are obtained from three different sets of experiments. *Inset* shows 20% SDS-PAGE of lysozyme (4.5 kDa) on the *left* and the 5-kDa fragment on the *right*. Gel was stained with Coomassie Brilliant Blue. *b,* binding isotherm of 5-kDa fragment (0.3 μM)-Ins(1,4,5)P_3 interaction (●) generated from spectrofluorometric titration.

sequence identity) to the Homer class of proteins from different mammalian sources. However, the region with 75% sequence identity lies outside the EVH1 domain, a subset of WH1 domain (28). The tertiary structure of WH1 domain is reported to have similarities with PH domain, well established for its phosphoinositide binding (29). Therefore, we carried out an alignment with available primary sequences of EVH1 domains (Fig. 13*b*). Two observations are noted from this result. First, the sequence shows greater than 30% homology with EVH1 domains. Second, among the different EVH1 domains, the sequence of the 5-kDa fragment shows maximum (41%) homology with EVH1 domains from Homer proteins only.

DISCUSSION

The validity of the fluorescence method to evaluate the ligand binding potential of phytase and its tryptic fragments is indicated from the fact that the values obtained from this method agree well with the results from a more direct binding method using radiolabeled ligand(s). The experimental observations could be summed up to the following conclusions. Dual functions of phytase can be attributed to two different sites in the protein. That is why the dual functions could be dissected in two tryptic fragments each with one function. Restoration of both activities by mixing the two fragments further supports this. The effect of saturation of the high affinity site with *myo*-inositol trisphosphate upon the catalytic potential of phytase is reflected from change in two parameters, namely dissociation constant for the substrate, $InsP_6$, and activity of the enzyme for the same substrate. The important and probably physiologically significant result is the demonstrated interaction between the two sites. We have also noticed that the interaction between the two sites is mutual. Another important observation follows from the homology search. They are discussed in detail below.

Alteration in the affinity of phytase for the substrate, $InsP_6$, upon saturation of the high affinity site with $InsP_3$ is clearly indicated from Table I. A comparison of the energetics shown in Table II further corroborates the conclusion. Although the entropy-driven nature of the phytase-$InsP_6$ association remains unaltered, values of all associated thermodynamic parameters change. It might occur as a result of *myo*-inositol trisphosphate-induced conformational change in the enzyme. A change in conformation has been indicated from earlier reports. This was concluded from the observed decrease in tryptophan accessibility of phytase, when it is saturated with *myo*-inositol trisphosphate at the high affinity site. Results from the present study have thrown light on the nature of the change. The association alters the conformation such that there is a reduc-

TABLE VII
Thermodynamic parameters for interaction of phytase or its tryptic fragments with ligands

Dissociation constants for 66-kDa fragment-$InsP_6$ and 5-kDa fragment-Ins(1,4,5)P_3 interactions were determined by spectrofluorometric titrations in 50 mM Tris-HCl buffer, pH 7.0. Concentration of tryptic fragment in these titrations was 0.3 μM. Dissociation constant for phytase-Ins(1,4,5)P_3 interaction at the high affinity site was evaluated at different temperatures from filter binding assay in 50 mM Tris-HCl buffer, pH 8.0. Free energy (ΔG) of the interaction is at 10 °C (Equation 5). Values for ΔH and ΔS are determined from van't Hoff plots of $\ln K_a$ versus $1/T$ (Equation 6 and 7). The data below represent mean of two sets of experiments.

Enzyme/tryptic fragment	Ligand	Thermodynamic parameters		
		ΔG	ΔH	ΔS
		kcal/mol		*e.u.*
Phytase	$InsP_6$	−5.8	+14.6	+71.9
66-kDa fragment	$InsP_6$	−6.2	+14.9	+74.6
Phytase	Ins(1,4,5)P_3	−9.0	−10.4	−4.9
5-kDa fragment	Ins(1,4,5)P_3	−9.0	−15.3	−21.7

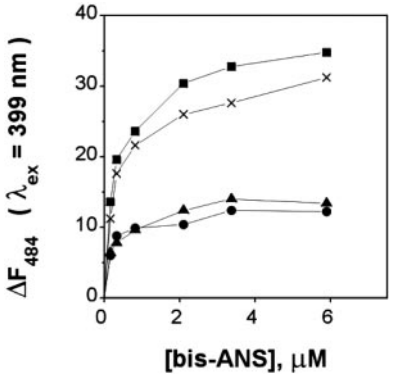

FIG. 12. **Fluorescence titration of phytase (0.3 μM) with bis-ANS (λ_{em} = 484 nm and λ_{ex} = 399 nm) in 50 mM Tris-HCl buffer, pH 7.0, at 15 °C under different conditions.** Phytase (0.3 μM) alone (■), preincubated with 2 mM $InsP_6$ (×), 2 mM $InsP_6$ plus 300 nM Ins(1,4,5)P_3 (▲), and 300 nM Ins(1,4,5)P_3 (●).

(a)

```
5 kD          ----------------------KRARTEYGRAAQ-----------------
Q9NSC1        TRNAELEHQLRAMERSLEEARAERERARAEVGRAAQLLDVRLFELSELREGLAR
Q99JP6        TRNAELEQQLRAMECNLEEARAERERARAEVGRAAQLLDVRLFELSELREGLAR
O95350        TRNAELEHQLRAMERSLEEARAERERARAEVGRAAQLLDVSLFELSELREGLAR
Q9Z2X5        TRNAELEQQLRAMESNLEEARAERERARAEVGRAAQLLDVRLFELSELREGLAR
Q9Z215        TRNAELEQQLRAMECNLEEARAERERARAEVGRAAQLLDVRLFELSELREGLAR
Q9NSC5        TRNAELEHQLRAMERSLEEARAERERARAEVGRAAQLLDVRLFELSELREGLAR
O14580        TRNAELEHQLRAMERSLEEARAERERARAEVGRAAQLLDVSLFELSELREGLAR
                                      *** * *****
```

(b)

```
5 kD        ------------------------KRARTEYG----------RAAQ-------------
1DDV        AIINSTITPNMTFTKTSQKFGQWADSRANTVYGLGFSSEHHLSKFAEKFQEFK-------
1QC6        VVINYSIVKGLKYNQATPTFHQWRDARQ--VYGLNFASKEEATTFSNAXLFAL-------
AAC71021    AIINSTITPNMTFTKTSQKFGQWADSRANTVYGLGFSSEHHLSKFAEKFQEFKEAARLAK
AAC71027    VIINSTITPNMTFTKTSQKFGQWADSRANTVFGLGFSSEQQLTKFAEKFQEVKEAAKIAK
                                    *: :::*           :
```

FIG. 13. **Sequence alignment of 12 amino acid residues from the N-terminal of the 5-kDa fragment.** *a,* Homer proteins. The proteins aligned are as follows: amino acid sequence of N-terminal 12 amino acids from the N-terminal of the 5-kDa tryptic fragment of phytase from *V. radiata*, *5-kDa*; Homer-3B protein from *Homo sapiens*, *Q9NSC1* (32); similar to Homer, neuronal immedia from *Mus musculus*, *Q99JP6*; Homer-3 from *H. sapiens*, *O95350* (31); Vesl-3 from *Rattus norvegicus*, *Q9Z2X5*; Homer-3 (fragment) from *M. musculus*, *Q9Z215* (31); Homer-3A flip protein from *H. sapiens*, *Q9NSC5* (32); and R27090_3 from *H. sapiens*, *O14580*. SWALL data base identity numbers are indicated. * represents identical amino acids in the various sequences. *b,* EVH1 domains. The proteins aligned are as follows: amino acid sequence of N-terminal 12 amino acids from the N-terminal of the 5-kDa tryptic fragment of phytase from *V. radiata, 5-kDa*; Homer EVH1 domain from *R. norvegicus*, Protein Data Bank code, *1DDV* (33); EVH1 domain in Ena/Vasp-like protein from *M. musculus*, Protein Data Bank code, *1QC6* (34); EVH1 domain in Homer-1a from *M. musculus*, GenBank™ accession number *AAC71021* (31); and Homer-2a from *H. sapiens*, GenBank™ accession number *AAC71027* (35). * represents identical amino acids, and **:** represents identical amino acids in four sequences out of the total of five. Sequences were aligned using the ClustalW program (36).

tion in the hydrophobic pocket in native phytase. That is why the extent of binding to bis-ANS undergoes a reduction along with a decrease in the fluorescence emission intensity of the extrinsic fluorophore. The conformational change, however, does not lead to any alteration in the secondary structure of phytase, because the far-UV CD spectra of phytase does not change significantly upon addition of *myo*-inositol trisphosphates (figure not shown).

The observed effect of the high affinity association upon the substrate binding potential of phytase is further substantiated by the kinetic data. It is clear that high affinity binding leads to an enhancement in the catalytic rate. Since the dephosphorylation reaction is sequential, we have restricted to a demonstration of the increase in apparent overall rate rather than a detailed analysis. These data support the conclusion that $InsP_3$ acts as an activator of phytase. Whereas 300 nM Ins(1,4,5)P_3/Ins(2,4,5)P_3 could activate the enzyme allosterically, 500 nM Ins(1,3,4)P_3 isomer could also induce the effect although to a lesser degree. This observation is consistent with the earlier reported trend in Ca^{2+} mobilization potentials of the three trisphosphate isomers (3).

We have carried out a detailed characterization of the two binding sites. For that purpose, tryptic digestion of the enzyme was performed successfully to show that the two functional sites are located at different positions. The ability of 66-kDa fragment to bind $InsP_6$ with 1:1 stoichiometry and hydrolyze the substrate indicates that the fragment contains the catalytic site. Lower hydrolyzing activity may be due to the absence of the other tryptic fragments, which might play a scaffolding role. Reconstitution studies also affirm that the presence of the remaining fragments of the enzyme is important for the hydrolyzing activity of the enzyme. The 5-kDa fragment is equally efficient as phytase in the mobilization of Ca^{2+}. Data in Tables V and VI also unequivocally suggest that the 5-kDa fragment is not an offshoot from the 66-kDa fragment. Stoichiometry (1:1) of the association of phytase/66-kDa or 5-kDa fragment with $InsP_6$ or Ins(1,4,5)P_3 (Table V) proves that the association is specific and the resulting function is an outcome of the association. Other important supporting information is the result that demonstrates that both consequences of the mutual interaction between the two sites of phytase occur even when we substitute phytase with an equimolar mixture of 66- and 5-kDa fragments (Fig. 8 and Table VI).

The results from the use of fluorescent probe, bis-ANS, imply that binding of the substrate occurs at the hydrophilic surface of the protein. Positive enthalpy change upon $InsP_6$ binding to phytase could originate from (i) electrostatic interaction between the arginine side chain and the phosphate groups and (ii) an energetically unfavorable conformational change in phytase. Both suggestions are in accordance with the reports on the crystal structure of *Escherichia coli* phytase and its complex with $InsP_6$ (30). The conformational change at the active site is necessary for the catalytic activity. Entropy increase, the prime factor leading to a favorable free energy change, originates from the release of bound water from the hydrophilic pocket of binding. $InsP_3$ binding to the high affinity site facilitates $InsP_6$ binding at the catalytic site. This occurs due to the fact that there is an alteration in the conformation of phytase. The altered conformation reduces the positive enthalpy change when phytase binds to $InsP_6$ in the presence of *myo*-inositol trisphosphates. The net result is an increase in the affinity constant.

On the other hand, the negative enthalpy change associated with $InsP_3$ binding at the high affinity site in the enzyme implies the role of hydrogen-bonding interaction and hydrophobic association. We do not have evidence for the former. Results with bis-ANS (Fig. 12) support the important role of hydrophobic association.

In conclusion, our observations suggest that the 66-kDa fragment houses the catalytic site and that the 5-kDa fragment contains the site for high affinity $InsP_3$ binding. The results suggest a domain structure in the enzyme.

Phytase is well known as an enzyme involved in the sequential degradation of *myo*-inositol hexakisphosphate. A novel feature of phytase reported is the high affinity association with $InsP_3$ leading to Ca^{2+} mobilization from microsomes/vacuoles. We have shown here that the 5-kDa tryptic fragment from phytase contains a single high affinity $InsP_3$-binding site, and

it can induce Ca^{2+} mobilization from microsomes/vacuoles. Therefore, we have carried out sequence and structural homology of the N-terminal amino acids of the 5-kDa fragment with different classes of proteins. As the results indicate, we have come across a significant homology with the Homer class of proteins. A recent report (31) has suggested that the Homer protein from brain forms a physical tether linking metabotropic glutamate receptors (mGluRs) and *myo*-inositol 1,4,5-trisphosphate receptor ($InsP_3R$), because these receptors co-immunoprecipitate as a complex with Homer from brain. The data further imply that phytase has the potential to participate in signaling pathway via formation of the ternary complex, phytase-$InsP_3$-$InsP_3R$. However, the sequence search does not preclude the existence of EVH1 domain in the 5-kDa fragment, although this appears to be remote as inferred from the poor homology observed with EVH1 domain, a subset of WH1 domain.

Physiological Significance—An important role of the phytase-*myo*-inositol trisphosphate-$InsP_3R$ complex in the cell will be to utilize $InsP_3$ generated by phytase (or different pathways) as an elicitor of intracellular Ca^{2+} efflux. It has been substantiated further that in the presence of neomycin which inhibits the phospholipase C activity responsible for generating $Ins(1,4,5)P_3$ from phosphatidylinositol 4,5-bisphosphate, initial regeneration of mung bean plantlet from the cotyledon explant is not inhibited (7). We have also noticed germination of mung bean seeds even when they are treated with LiCl, which has been established to shut off the pathway of generation of $Ins(1,4,5)P_3$ from phosphatidylinositol 4,5-bisphosphate. The growth is, however, less than that of the seeds grown in its absence. It may also be noted that there is an increase in the level of phytase during germination of seeds. Phytase dephosphorylates $InsP_6$ to produce isomers of *myo*-inositol trisphosphates. We have demonstrated that these isomers are capable of Ca^{2+} mobilization, thereby triggering the Ca^{2+}-dependent signaling during germination. Here, we have also shown that $InsP_3$ produced from the dephosphorylation of $InsP_6$ leads to an enhanced rate of dephosphorylation. Finally, our present results further support an alternate (salvage) pathway for Ca^{2+} mobilization during germination of the seeds (7).

Acknowledgment—U. P. and D. D. thank Professor (Dr.) N. Shimamoto, National Institute of Genetics, Mishima, Japan, for help in the sequence determination of the peptide.

REFERENCES

1. Mandal, N. C., and Biswas, B. B. (1970) *Plant Physiol.* **45,** 4–7
2. Mandal, N. C., Burman, S., and Biswas, B. B. (1972) *Phytochemistry* **11,** 495–502
3. Dasgupta, S., Dasgupta, D., Sen, M., Biswas, S., and Biswas, B. B. (1996) *Biochemistry* **35,** 4994–5001
4. Berridge, M. (1993) *Nature* **361,** 315–325
5. Shears, S. B., Parry, J. B., Tang, E. K. Y., Irvine, R. F., Michell, R. H., and Kirk, C. J. (1987) *Biochem. J.* **246,** 139–147
6. Drobak, B. K. (1992) *Biochem. J.* **288,** 697–712
7. Biswas, S., and Biswas, B. B. (1996) *Subcell. Biochem.* **26,** 287–316
8. Kammermeier, P. J., Xiao, B., Tu, J. C, Worley, P. F., and Ikeda, S. R. (2000) *J. Neurosci.* **20,** 7238–7245
9. Saio, K. (1964) *Plant Cell Physiol.* **5,** 393–400
10. Fiske, C. H., and Subbarow, Y. (1929) *J. Biol. Chem.* **81,** 629–636
11. Lowry, O. H., Rosebrough, N. J., Farr, A. L., and Randall, R. J. (1951) *J. Biol. Chem.* **193,** 265–275
12. Bradford, M. (1976) *Anal. Biochem.* **72,** 248–252
13. Chen, P. S., Toribara, T. Y., and Varner, H. (1956) *Anal. Biochem.* **28,** 1756–1758
14. Banik U., and Ray, S. (1990) *Biochem. J.* **266,** 611–614
15. Bitar, K., and Reinhold, J. G. (1972) *Biochim. Biophys. Acta* **268,** 442–452
16. Yang, W., Matsuda, Y., Sano, S., Masutani, H., and Nakagawa, H. (1991) *Biochim. Biophys. Acta* **1075,** 75–82
17. Wang, J. L., and Edelman, G. H. (1971) *J. Biol. Chem.* **246,** 1185–1192
18. Lakowicz, J. R. (1983) *Principles of Fluorescence Spectroscopy*, pp. 258–297, Plenum Publishing Corp., New York
19. Lehrer, S. *S*., and Leavis, P. C. (1978) *Methods Enzymol.* **49,** 222–236
20. Castellan, G. W. (1989) *Physical Chemistry*, pp. 277–294, Narosa Publishing House (Indian Student Edition), New Delhi, India
21. Mazorow, D. L., and Millar, D. B. (1990) *Anal. Biochem.* **186,** 28–30
22. Grynkiewicz, G., Poenie, M., and Tsien, R. Y. (1985) *J. Biol. Chem.* **360,** 3440–3450
23. Pearson, W. R., and Lipman, D. J. (1988) *Proc. Natl. Acad. Sci., U. S. A.* **85,** 2444–2448
24. Orengo, C. A., Michie, A. D., Jones, S., Jones, D. T., Swindells, M. B., and Thornton J. M. (1997) *Structure* **5,** 1093–1108
25. Holm, L., and Sander, C. (1998) *Nucleic Acids Res.* **26,** 316–319
26. Maitra, R., Samanta, S., Mukherjee, M., Biswas, S., and Biswas, B. B. (1988) *Indian J. Biochem. Biophys.* **25,** 655–659
27. Dasgupta, S., Dasgupta, D., Chatterjee, A., Biswas, S., and Biswas, B. B. (1997) *Biochem. J.* **321,** 355–360
28. Niebuhr, K., Ebel, F., Frank, R., Reinhard, M., Domann, E., Carl, U. D., Walter, U., Gertler, F. B., Wehland, J., and Chakraborty, T. (1997) *EMBO J.* **16,** 5433–5444
29. Prehoda, K. E., Lee, D. J., and Lim, W. A. (1999) *Cell* **97,** 471–480
30. Lim, D., Golovan, S., Forsberg, C. W., and Jia, Z. (2000) *Nat. Struct. Biol.* **7,** 108–113
31. Tu, J. C., Xiao, B., Yuan, J. P. Lanahan, A. A., Leoffert, K., Li, M., Linden, D. J., and Worley, P. F. (1998) *Neuron* **21,** 717–726
32. Soloviev M., Ciruela F., Chan, W. Y., and McIlhinney, R. A. J. (2000) *J. Mol. Biol.* **295,** 1185–1200
33. Beneken, J., Tu, J. C., Xiao, B., Nuriya, M., Yuan, J. P., Worley, P. F., and Leahy, D. (2000) *Neuron* **26,** 143–154
34. Fedorov, A. A., Fedorov, E. V., Gertler, F. B., and Almo, S. C. (1999) *Nat. Struct. Biol.* **6,** 661–665
35. Xiao, B., Tu, J. C., Petralia, R. S., Yuan, J. P., Doan, A., Breder, C. D., Ruggiero, A., Lanahan, A. A., Wenthold, R. J., and Worley, P. F. (1998) *Neuron* **21,** 707–716
36. Thompson, J. D., Higgins, D. G., and Gibson, T. J. (1994) *Nucleic Acids Res.* **22,** 4673–4680